ADVANCED FUNCTIONAL MATERIALS
www.afm-journal.de

Materials Views
www.MaterialsViews.com

Nano Molecular-Platform: A Protocol to Write Energy Transmission Program Inside a Molecule for Bio-Inspired Supramolecular Engineering

Subrata Ghosh, Mrinal Dutta, Satyajit Sahu, Daisuke Fujita, and Anirban Bandyopadhyay**

In a coded self-assembly, a simple code is written in the molecule, which self-assembles the molecules into a fractal like structure, which acts as a seed for the next step. As the molecule turns into a complex seed, the code transforms into another form and several seeds self-assemble into another structure, which acts as a seed for the next step. Until now, this technology was considered as a prerogative of nature. Here, a dendritic network is used to write a basic code by synthetically attaching 32 molecular rotors and doping two controller molecules in its cavity. The code live, which is an energy transmission path in the molecule, is imaged. When the energy transmission path or code is triggered, a series of products generate one after another spontaneously. Two examples are: i) dendritic seed (5–6 nm)→paired nanowire (≈12 nm)→nanowire (≈200 nm)→microwire (500 nm)→wire like rod (1–2 μm)→jelly→rectangular sheet (5 μm). ii) dendritic seed→nano-sphere (20 nm)→micro-sphere (500 nm)→large balls(1 μm)→oval shape rod (5–10 μm)→Y, L or T shaped rod assembly. The energy level interactions are tracked using spectroscopy how exactly a directed energy transfer code generates multi-step synthesis from nano to the visible scale.

1. Introduction

The adventure of molecular machines[1,2] will not remain confined in replicating day-to-day used machine-analogues.[2] Ensuring an accurate translation of work as programmed in the atomic arrangement via multi-level switching[3] would revolutionize the automated manufacturing of giant structures. The collective organizational behavior of biological molecular machines[4] is the key to the construction life forms and the transition of codes occurs from a few nanometers to the meter scale. The biological code uses fractals as part of its structuring into material form, however, the codes transforms at every step of self-assembly and it takes a complete new form during the growth. Therefore, it is a multistage growth process; at each stage, the same code generates a new structure. We cannot carry out high precision manipulation at the atomic scale using global energy sources like laser light, magnetic or electric field. To resolve this issue we argued for a nano-platform[5] and an associated computing.[6] Here, we advance the nano-platform concept by discarding the old perception that dendrimers are dynamically random and cannot produce an organized potential fluctuation essential for molecular programming.

2. Results and Discussion

We attached 32 molecular rotors (MR)[1] radially around the dendritic network to screen internal dynamics and regulate the random fluctuation in dendritic pathway.[7–10] Screening a dendrimer from its environment is considered a critical issue.[11–14] In addition to rotor dynamics, screening is associated with the synchronized energy transport between rotors (MR) and doped controller. Synchronization ensures a noise-free energy transport between two energy levels, however, it is an unfamiliar potential of a dendritic box,[15] which enables us to look beyond the unitary objective of dendrimer as drug delivery agent.[3] By tuning the energy transport[10] selectively between the rotor and the controller, we could lock the system at any particular point on the dynamic path, and each path could trigger a particular kind of self-assembly. In our system, "if" dynamics A is triggered, "then" A triggers a set of B dynamics and the self-assembly starts. This is similar to one "if-then" argument used in a software programming. Thus, we could encode multi-channel energy transmission pathways or several "if-then" arguments inside a single dendritic molecule—it is more explicit multi-channel control than the theoretical predictions.[7,8] First it triggers controller and rotor molecules only, then, four dendritic lobes interact as distinct potential units (**Figure 1**a). At multiple stages, several distinct dynamics of entire system are activated—hierarchical dynamics govern the hierarchical structures.[16–19] Due to screening, the

S. Ghosh, D. Fujita, A. Bandyopadhyay
Nano Characterization Unit
1–2–1 Sengen, National Institute for Materials Science
Tsukuba, Ibaraki, 305–0047
E-mail: ocsgin@gmail.com; anirban.bandyo@gmail.com
M. Dutta
International center for Materials
and Nano-architectronics (MANA), 1–1 Namiki, 305–0044, Japan
S. Sahu
Indian Institute of Technology
Rajasthan, Bio-inspired System Science
Jodhpur, India, 342011

DOI: 10.1002/adfm.201302111

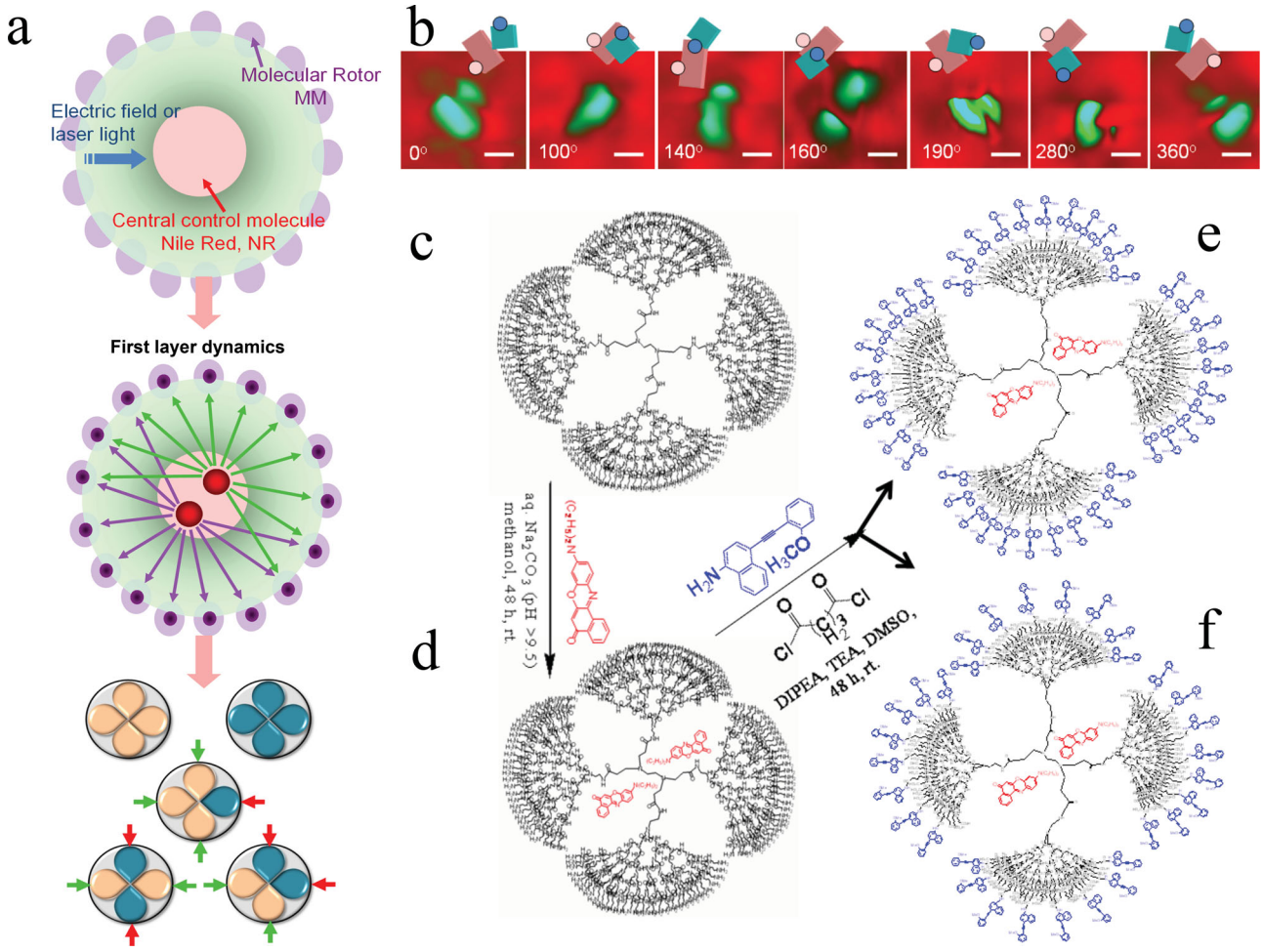

Figure 1. a) Schematic design of 3D molecular platform PCM, light or electric field excites NR (top), in the first layer dynamics, NR excites all MR around the surface (middle) and the second layer dynamics starts when four dendritic lobes adopt five distinct symmetries based on potential differences shown in two different colors (bottom). Two arrows demonstrate vectors of relative potential interaction among different regions. b) STM image of molecular rotation (blue molecular structure in panel (d), OCH_3 is blue ball, NH is red ball in the schematic to follow rotation) at 77K, 50 pA, 2 V on Si(111) surface, we demonstrate controlled rotation by decreasing temperature below freezing temperature and thermal noise of STM tip was used to induce noise and associated rotation, at 300K, molecule rotates so fast that this study cannot be done, scale bar is 0.5 nm. c) PAMAM dendrimer doped with NR (red) dye, we get panel (d). From panel (d), we carry out amidation reaction with molecular rotor (MR, shown in blue). We get DMSO soluble 42 MR connected derivative in panel (e) and another, water soluble 32 MR connected derivative in panel (f), namely PCM. We use PCM for building the structures.

potential lobes switch among four choices, delivering products with sizes bellow 7 nm to a few millimeters. Thus, a directed energy exchange[20] in the dendrimer's many-to-one network generates a distinct potential symmetry in the four lobes. Transition of this symmetry means switching of dynamics, which triggers a new self-assembly.

We started synthesis with PAMAM dendrimer, dope Nile Red (NR) molecule inside the structural cavity to make a dendritic box and then attached 32 molecular rotors (MR) outside the PAMAM sphere. We used a short form P for PAMAM, C for controller NR molecule and M for molecular rotor, thus the desired product is PCM. Theoretically, we worked on various design aspects to find a suitable rotor molecule that works when attached to the PAMAM surface. The final molecule uses available energykT to perpetually rotate its two planes by 360° one opposite to another above 280 K, around the triple bond junction (Movie 1, Supporting Information). By temperature variation scanning tunneling microscope (STM) study (Figure 1b), we have identified that the molecular rotor starts rotating[21] beyond threshold energy, irrespective of the nature of the energy. For example, we could rotate it via electric field, as shown here, and if we increase the temperature, the similar rotation emerges. This is the foundation of our rotor control. Here we provide a summary of the three-step synthesis process of this molecular rotor and the synthetic challenges of PCM (Figure 1c,d,e) is described in the methods summary and in the supporting information online (text and Figures S1–S4, Supporting Information).

The most challenging aspect to study our "programming" protocol is to explicitly underpin the energy transmission

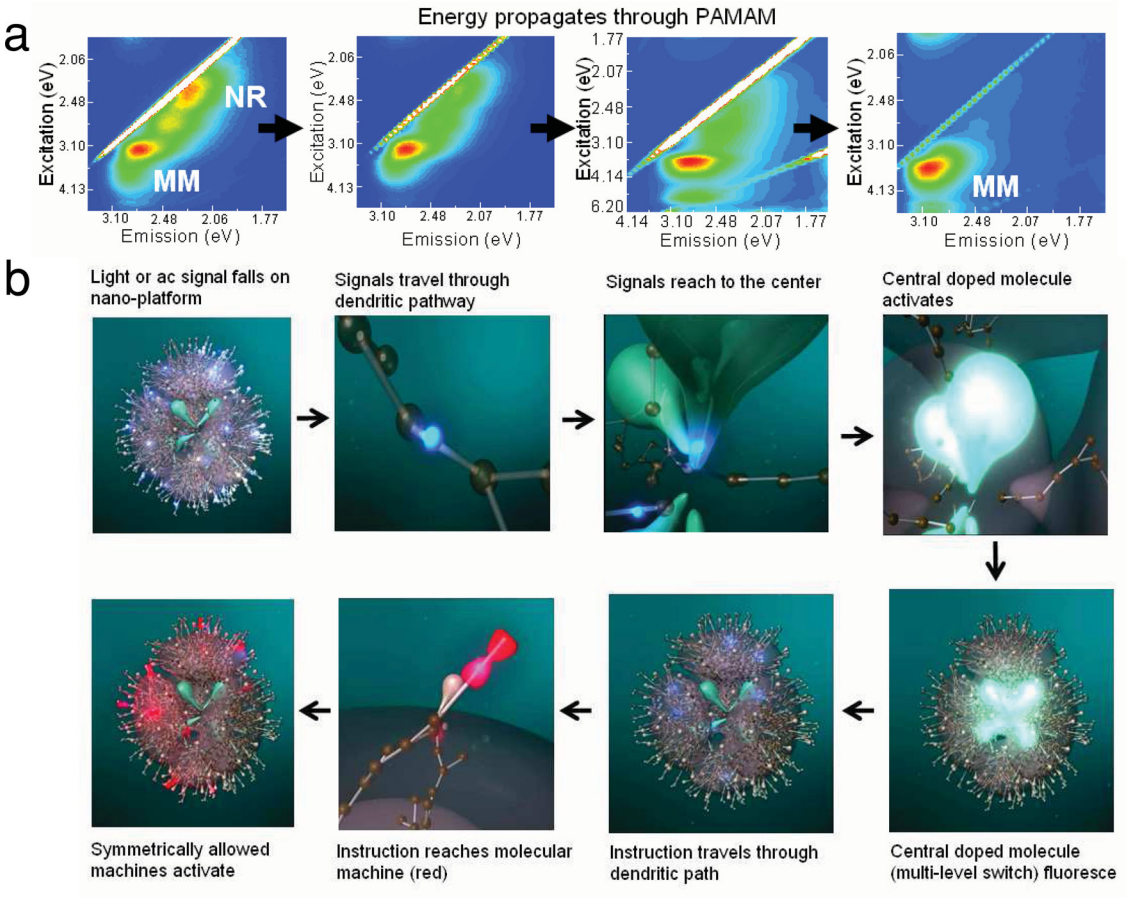

Figure 2. a) Nile Red (NR) and Molecular rotor's (MR) contribution are identified in the CEES spectrum, with density modulation we demonstrate how environmental changes could precisely tune energy transmission inside PCM structure. b) Schematic kpresentation of central control molecule (Nile Red) shown as sea-green colored light-bulb, and dumb-bell shaped red colored molecular rotor communicates by soliton, theoretical simulation is presented as series of pictures to explain panel (a).

pathways between different molecular parts of PCM, for which a suitable characterization tool does not exist. Using combined excitation and emission spectroscopy (CEES),[22–24] we have identified an energy transfer pathway between the molecular rotor and the doped central control molecule MR↔PAMAM↔NR. In 3D CEES study, the fluorescence intensity is plotted as a function of excitation and emission energy. Since each peak maps the energy transitions, a 3D CEES map covers multiple simultaneously operating pathways. Earlier, this technique was used to identify the energy transfer protocols between doped rare earth metal and the solid-state semiconducting architectures. We have measured CEES for NR and MR molecules separately, the peaks characteristic of NR and MR are at around 2.45, 2.35 eV (E_x,E_m) and at 3.14, 3.72 eV (E_x,E_m). Comparing isolated component's spectra with the derived compound data, we measure peak-shifts, creation/disappearance of peaks reveal how individual molecular parts interact when bonded weakly/strongly to the supramolecular architecture. In PCM's CEES spectrum we identify MR's peak, and find extremely long (≈1 s) relaxation time therein, so we conclude, MR works as freely rotating ligand on the PCM surface. In **Figure 2**a and SS1 (Supporting Information), we demonstrate that in the final product PCM, the CEES peak for NR, that appears initially, shifts gradually to the peak location of MR, exactly as shown schematically in Figure 2b. Now, it means that when an external energy is imparted to PCM, first, it controls the energy transmission of the NR and then the energy is transported towards the molecular rotor via PAMAM matrix. One transition "if" triggered, "then" another transition is automatically activated, this is how an argument is written in a software program so we call it "molecular programming". Thus, CEES provides exact details of the band level transitions that triggers the formation of the supramolecular architectures, and by matching the band energy with the molecular dynamics we could correlate the particular dynamics of a functional group responsible for the architecture formation (**Figures** 2a,**3**a–c,**4**a). It is important to note that the choice of molecular components, like Nile Red and rotor were made by studying several alternate structures. Only those molecules, which after combining with the PAMAM matrix, deliver an accurate energy transfer following the desired pathway should be selected only. For example, Rose Bengal molecule did not exhibit the kind of programmed energy transfer in this case.

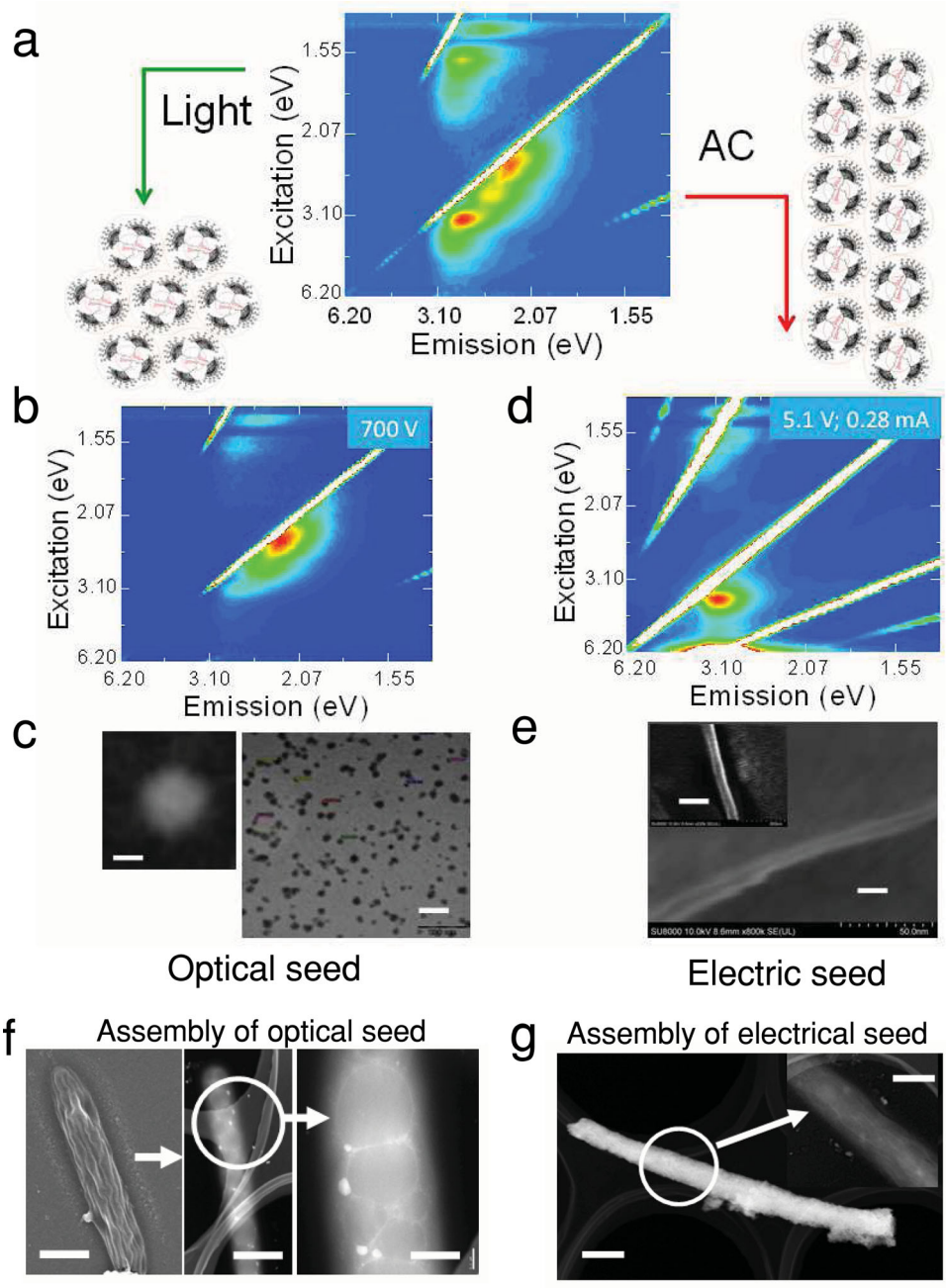

Figure 3. a) CEES spectra of PCM, when light (700V) or AC/DC electric bias (5.1 V, 0.28 mA) is applied, individual PCMs assemble as shown schematically, and CEES spectrum changes to panels (b,c) AFM images of panels (b,c) are shown below in panels (d,e) respectively. Paired nanowire and sphere is zoomed in the smaller panels. Scale bar for panel (d) 120 nm and 14 nm (zoomed); for panel (e) 20 nm and 30 nm (zoomed). f) Optical seeds (spheres) naturally assemble into rice-seed like structure (left, SEM image, scale bar 200 nm), we have zoomed these structures in TEM, and could resolve the spherical balls inside (scale bar 190 nm). g) Electrical seeds (nanowire) naturally assembles into a ≈10 µm long rigid rods, scale bar of SEM image is 400 nm, we have zoomed these structures in TEM, and could resolve the nanowires inside (scale bar 380 nm).

Figure 3 shows two self-assembly experiments. First, applying an ac and a dc electric field in the PCM solution to generate: PCM→nanowire→microwire→wire like rod→jelly→rectangular sheet. Second, varying the laser power exposed to the PCM solution to generate a photon induced architectures: PCM→nano-sphere→micro-sphere→large balls→oval shape rod→Y, L or T shaped rod assembly. For the first experiment, we put two Sn electrodes in the cuvette and cables are taken out of the measurement set up. Using these cables, we send dc bias starting from 30 mV to 10 V and ac signal from 1 Hz to 50 MHz and varying the ac bias 30 mV_{rms} to 5 V_{rms}. For the optical experiment only laser light was exposed from outside. When we increase the electric dc bias to ±2V, we observe white colored thin wires form in the solution. Beyond

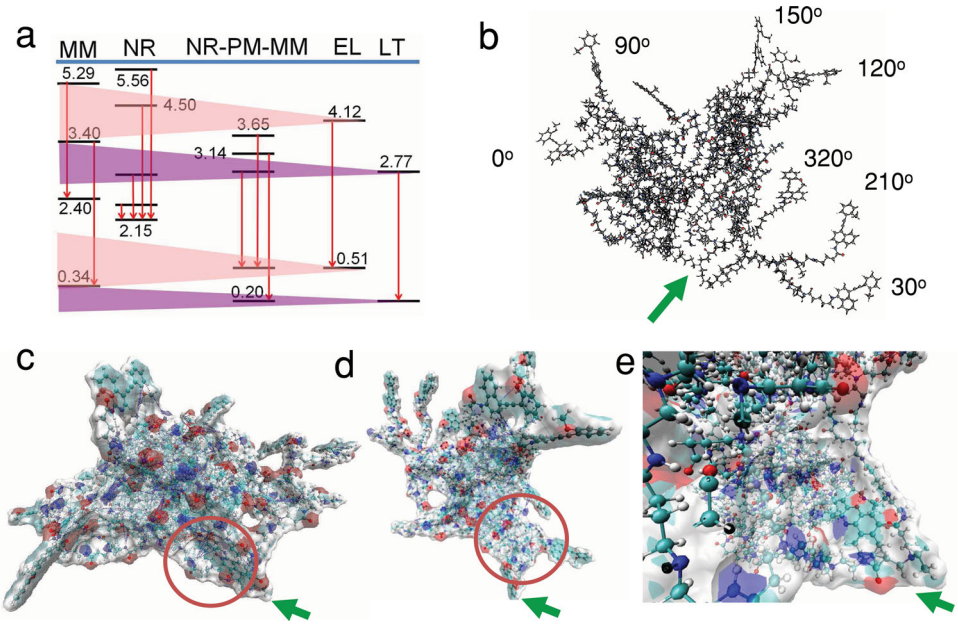

Figure 4. a) Energy levels of molecular rotor (MR), Nile red (NR), PCM or the NR-PAMAM-MR molecular architecture, electric field produced nanowire pair EL, and the light induced sphere LT (all values are in eV). Allowed transitions are shown with an arrow. These data are experimentally determined from the CEES spectrum of the five individual materials. From the energy level diagram it is clear how NR and MR contributes to the nanowire and nano-sphere formation. It should be noted that PAMAM does not have any energy levels in this domain, however, in the NR-PM-MR column we see that 3.14 eV, 2.77 eV, and 0.51 eV are three energy levels which contributes to the communication between NR and MR. Shadow shows the energy level convergence route during supramolecular assembly formation. b) A single branch of NR-PAMAM-MR molecular architecture, relative rotation of the molecular rotor is shown with an angle. c,d) two different angular views of panel (b), energy minimized, solvent accessibility, electrostatic potential (red positive, blue negative), H bonding are shown in the plots, the NR doping is enlarged in panel (e). Cavity with NR is depicted with red circle, green arrow shows beginning of the branching.

a threshold density, these wires form microwires, which construct millimeter or centimeter scale wires. Some of these wires while floating in solution form rods, which combine just like a jelly and precipitates in the form of a rectangular sheet. All CEES peaks of PCM disappears in the PCM based nanowires and only 3.52 eV, 4.12 eV (E_m,E_x) peak survives. We drop the solution on a SiO_2 substrate and Cu grid to study its structure formation via high resolution SEM, EDX, and TEM. In case of TEM study, Pt was deposited on the film prior to imaging (Figure 3d,e,g). PCM first forms 15 nm wide pair of nanowires, one connecting to another. The derived architecture is shown with a schematic. Almost, always, we found additional 200 nm × 1 μm nanowires made of giant PCM structures formed naturally during synthesis and TEM image carries clear evidence of hierarchical/multilayered assemblies (Figure 3g).

For the laser induced self-assembly (Figures 3b,c,f), we use fresh PCM solution and increase the laser pulse power to 5 mW. Beyond this threshold, first an optical seed forms which assembles continuously into larger sized spheres, which eventually forms oval shaped rods (Figure 3f). The rods also self-assemble into a complex pattern and precipitates. When optical seed forms, we find that similar to the case of electric bias induced self-assembly, all the CEES peaks disappear except the 2.53 eV, 5.31 eV (E_m,E_x) peak. This striking similarity between optical and electrical structural transformation tells us that fundamentally, the entire self-assembled architecture be it nanowires or sphere behaves as two distinct basic structural units. We isolate the reaction material from solution and characterize it with SEM, EDX, and TEM. Inside a supramolecular sphere, we found that there are 10 PCMs around a single PCM molecule, which renders it a sphere shape. A schematic of this architecture is shown in Figure 3a. The CEES spectra and non-linear emission intensity variation as function of laser power suggests that the sphere and the nanowire generate a sharp and intense emission at a very particular emission frequency. The nonlinear intensity increase as function of input power suggests that both the structures might act as an optical cavity.[25–29] The CEES spectrum reveals that during the structural transformation from isolated PCMs to a nanowire or sphere, the nanowire like supramolecular architecture requires 1.43 eV more energy than the sphere like architecture formation. The nanowire is formed as 3.40 eV (S_2) band of MR is triggered while the sphere is formed as 3.65 eV (S_1) band of MR is triggered by the central NRs, therefore, electric field and laser power controls the fundamental energy level transitions to define the eventual architecture symmetry.

In order to further confirm the role of NR in triggering the MR's decisive energy levels, we created a PCM structure without doping the NR molecule inside. Then we failed to create any of these supramolecular architectures, even intermediate PAMAM peaks also disappear, which proves that the central doping by NR is essential to accurately trigger the MR's decisive energy levels that govern the nucleation of hierarchical supramolecular assemblies. We have also designed and synthesized several PCM like seed structures by attaching molecules other than MRs, on the PCM surface neighboring

the MRs to cover more of the open amine ends of the PAMAM dendrimers. However, all attempts to modulate the supramolecular assemblies failed, thus, the directed energy transfer is a critical issue. In summary, three features establish the NR's direct role in the energy transfer process of PCM. First, as soon as the free amine end groups of PAMAM are covered with any other molecules, the band transitions in CEES disappear even though the NR molecules are inside. In these cases, we could not generate any optical or electronic field induced megamer[30] structures. Second, Figures 2a and SS1 (Supporting Information) show how exactly NR dominated band-level-transitions shift to MR dominated transitions, which is a direct evidence of selective energy transfer that controls the selection of the kind of architecture to be created. Third, in the Figure SS4 (Supporting Information), which is an analytical version of Figure 3, we could see that NR activates the PAMAM matrix, and a very specific band corresponding to this transition[8] is visible here responsible for the sphere formation, while, the NR band completely disappears for the paired nanowire formation. Three versatile controls of NR that modulate the energy-transfer-process are: first, NR-band-control by an external molecule; second, gradual, linear, directive energy transfer[10] between NR and MR; third, structure-selective energy transfer by NR directly establish that NR interacts with the molecular parts in its vicinity at the energy level.

We replaced the NR molecule with Xanthene dyes, but the resultant PCMs did not provide interesting architectures eventually, but that failure taught us a very interesting principle of energy communication. It is essential to check the energy band order similar to NR-PAMAM-MR (2.57,2.77; 2.77,3.14; 3.14,3.65 eV E_m,E_x, Figure 4a) case. This particular energy level transition relationship also means the necessity of an energy gradient, which has always been argued for the dendritic energy transport.[10] Therefore, the choice of component is restricted and sometimes, the entire system needs to be discarded if the matching turns impossible. In future, more complicated atomic level programming with simultaneously co-existing multiple energy level pathways would very much be possible.[10] Another important aspect is the necessity of the multiple distinct dynamics of MR, because of which Nile Red could switch[21] specific ways[8] to initiate two rotations along with the PAMAM vibration, which helped MRs to couple with its neighbors to form giant structures. In the STM images of the molecular rotor, we have demonstrated these dynamics, and Figure 4 demonstrates the existence of multiple energy levels through which the energy relaxations could occur. Therefore, a proper design of the MR is essential so that its dynamics is tuned by the chained energy transfer process (note that 2.77 eV and 3.14 eV is common in NR-PAMAM-MR transition) with the doped molecule, which is an essential factor to build supramolecular architectures following multi-functional programming introduced here.

3. Conclusions

For two reasons we concluded that there does not exist any chemical bonding when PCM forms supramolecular assembly. First, we failed to find any reactive functionality in PCM that could lead to any chemical reaction. The MR part that is extended outside one PAMAM dendrimer cannot cross–react to the other PCM in its neighborhood[31] 32 in the supramolecular assembly. To be specific, PAMAM unit's left-out COOH groups are non-reactive to MR's free part, if those were active, the basic PAMAM-MR architecture PCM would never have formed at the first place. Second, in Figure SS5 (Supporting Information) we provide FTIR data for the paired nano-wire to confirm that it is identical to the FTIR data for the rotor-PAMAM bonded PCM, no new peak is generated when several single units combine to construct the final compound. Thus, covalent bonding does not exist, if it were, it should have created additional vibrational peaks in the FTIR or Raman spectrum.

Since both electronic and optical structures are stable, we have carried out molecular dynamics simulations to understand the physical locking of functional groups. The molecular simulation shows that the vibrational dynamics of four PAMAM lobes could generate five local potential energy minima.[9,16] In which if two MRs from two neighboring PCMs come in contact,[16] then, due to natural rotation of these rotor molecules they could lock themselves, either via OCH_3 or by the coupling of upper plane into one unit. Notably, OCH_3 locking stops the associated band transitions (Figure 4a). Thus, for spheres, the peaks specific to MR emission disappear in the CEES spectra, and the shrinking of long emission relaxation time suggests that not only the OCH_3 group, rather, entire upper plane of molecular rotor is blocked, enabling the NR emission to supersede the MR emission. Semi-empirical simulation of molecular dynamics[8] suggests that a few molecular rotors could lock two PCMs side by side too due to the field-induced organization. Then, the emissions due to NR is absorbed by the PCM network and as a result it disappears from CEES by enhancing the PAMAM's interaction band, finally, only the emissions due to MR dominates in the CEES spectrum. Figure 4b shows the emergence of several distinct dynamics of molecular rotor naturally, which consolidates our "locking mechanism" noted above. Frequency modulated energy transmission study[10] suggests that the optical field induced energy transfer generates a homogeneous oscillation of the PAMAM matrix as shown in Figure 4c,d. Its four lobes divide energy nearly similarly, which leads to the formation of a PCM-sphere. However, the electrical field induced transition induces a bipolar oscillation of PAMAM[16] at ≈300 K, bipolar means two PAMAM lobes get more energy than the other two, which causes the formation of a paired-nanowire (Figure 1a). Thus, the NR triggers MRs energetically that is the first layer dynamics exactly as shown in Figure 4e (note the electrostatic interaction shown in red and blue color). In the second phase, the PAMAM lobe potential fluctuates as distinctly visible in Figure 4c,d (red-blue pathway). Since these are sequentially coupled events, entire sequence resembles to the "if-then" statements written in a computer algorithm.

While generating a series of architectures, multiple dynamics are involved at different stages of self-assembly. Even though one stage produces the start-up seed for the next stage, the entire process of growth is confined within a very particular kind of energy level transition. Both external (light and electric field) and internal controls (NR-rotor transmission path) interplay in a much more complex manner than simple energy transmission associated dynamics. When a particular energy

level transition is maintained throughout successive self-assemblies, the self-similarity of interaction ensures a fractal nature of growth visible in SEM or TEM. Fractal seeds require constant rule for energy transfer. In future, if we similarly correlate fractal, energy level transition and the dynamics, we would program much more complex nano-to-centimeter scale assembly in the molecular structure itself.

4. Experimental Section

General synthetic protocol: Before synthesizing the PAMAM-MR complex, we dope the NR dye molecule inside the PAMAM 5.0 dendrimer cavities.[33] Since this process is highly pH dependent,[34] we optimized the pH for doping two NR molecules in one PAMAM, for NR, doping more than two molecules was not possible. After varying different solvents, elevated temperatures, pH etc., it is found that at >pH 9.0 the NR molecules get encapsulated inside the dendritic cavities at 300 K. The optimization process and all other synthetic characterization details are in the supporting information online text along with Figure S5 (Supporting Information) where we have plotted the number of NR from mass variation data of PAMAM versus NR-PAMAM along with the pH of the solution. Then we attach the MR molecule with the PAMAM molecules. In the FTIR spectrum of the PAMAM dendrimer attached with MR molecule in the Figure SS2 (Supporting Information), we see the peak corresponding to –C≡C– (≈2346 cm^{-1}), and an enhanced NHCO peaks (NHCO has two peaks ≈1536 cm^{-1} and ≈1656 cm^{-1}, before MR attachment ≈1656 cm^{-1} has more intensity than ≈1536 cm^{-1}, and after MR attachment this is just the reverse), which clearly carries the signature of the rotor MR attachment to PAMAM. Corresponding MALDI-TOF[35] and NMR studies were also performed to confirm the bonding.

Once the basic dendritic seed structure is synthesized after doping NR and connecting MRs, we found two different byproducts that are formed naturally during the synthesis process. We have isolated and characterized both the structures in details using quantitative MALDI-TOF, and counted the number of MRs connected to the surface (Figure S6, Supporting Information). In Figure SS3 (Supporting Information), we provide MALDI-TOF data after GCM, however, it should be noted that the broadening of the mass peak is natural for higher mass materials. Interestingly, one derivative with 32 rotors is water-soluble and the other derivative where 42 out of 128 open amine ends of PAMAM dendrimer are connected is not water soluble. The most probable homogeneous distribution of the MRs on the PAMAM surface generates two distinct kinds of crystalline profile, one has 3:1 surface coverage of amines, while the other has 4:1 coverage. For the 32-MR case, 3 amines are open, and the one at the center of the triangle is attached by a MR. Since thirty-two water insoluble MRs could not modify the solubility of the PAMAM surface, we get a water-soluble part. We isolated and used the water-soluble part for building the supramolecular structures, and by PCM, we always refer to this particular byproduct.

Even though we did not find any evidence of strong covalent bonding via FTIR or Raman studies, the supramolecular assembly exhibits extreme survival possibly only via physical bonding. We varied different control parameters like electric bias, ac and dc signal pumping, temperature variation, pH variation, sonication, however, the structures do not dissolve and switch it back to the initial form. During SEM experiment, we sent intense beam but could only isolate two nanowirespartially, however, there was no sign of any degradation of the nanowires, no sign of breaking or isolation into individual PCM spheres.

Mass spectroscopy directly provides us that 10 PCMS construct the supramolecular ball. In addition, SEM and TEM images clearly show the sphere diameter, from which number of PCMS are calculated using simple geometric rules. Total diameter of the ball gives us total volume of say n number of PCMs, then if we divide it by the volume of one PCM, we get the value of n.

Synthesis Protocol for NR Incorporation to PAMAM G5 Dendrimer: 40 mg (0.0015 mmol, 1 mL methanol solution is pipette out) of [PAMAM G5.0 (-NH_2)x] dendrimer (*m*/*z* 26000 Da) is taken into a glass vial containing a magnetic bar and 1 mL methanol and 1 mL aqueous sodium carbonate (pH > 9.5) are added. The solution is stirred well and 10 mg solid crystal of Nile-red (molecular weight ≈318.3 Da) is added in excess, the solution is allowed to stir for 2 days at room temperature (≈22–25 °C).

After 2 days of continuous stirring, the solution is concentrated by removing methanol under vacuum and the aqueous solution is filtered, the filtrate is then dialyzed through cellulose parchment. The aqueous solution is washed with ethyl acetate and dichloromethane with mechanical shaking several times until the organic layer becomes completely colorless that ensures the complete removal of all weakly bind Nile-red on the dendrimer surface. After removal of the solvent, the product obtained (yield 99%) is Nile-red encapsulated PAMAM dendritic box which we call as PCM.

Synthesis Protocol for MR Attachment on {NR Encapsulated PAMAM G5 Dendrimer}: 20 mg [PAMAM G5(-NH_2)$_x$-NR] is taken into 2 mL of dry DMSO and then we add a mixture of 42 mg (excess) of MR in 1 mL DMSO, 1 mL of TEA (Et_3N) and 1 mL of DIPEA (iPr_2EtN) and stirred for 5 h. Then 100 µL of glutaryl chloride is added very slowly within a time period of 10 min. at ice-water temperature and the mixture is allowed to stir for 2 days at 300 K. Finally, the mixture is dialyzed through cellulose parchment in Milli-Q water for 24 h to get a final PCM. If MRs are connected to the PAMAM surface before NR doping, it is very difficult to dope the NR afterwards.

Supporting Information

Supporting Information is available from the Wiley Online Library or from the author.

Acknowledgements

This work was supported by NIMS Sengen-site (Nano Innovation Center), Inamori Foundation, JSPS Grants in Aid for Young Scientists (A) for 2009–2011, Grant number 21681015 (Govt. of Japan).

Received: June 21, 2013
Revised: August 27, 2013
Published online: October 9, 2013

[1] N. Koumura, R. W. J. Zijlstra, R. A. van Delen Delen, N. Harada, B. L. Feringa, *Nature* **1999**, *401*, 152–155.
[2] Y. Shirai, A. J. Osgood, Y. Zhao, K. F. Kelly, J. M. Tour, *Nano Lett.* **2005**, *5*, 2330–2334.
[3] S. Galeazzi, T. M. Hermans, M. Paolino, M. Anzini, L. Mennuni, A. Giordani, G. Caselli, F. Makovec, E. W. Meijer, S. Vomero, A. Cappelli, *Biomacromolecules* **2010**, *11*, 182–186.
[4] R. D. Astumian, *Nat. Nanotechnol.* **2012**, *7*, 684–688.
[5] A. Bandyopadhyay, S. Acharya, *Proc. Natl. Acad. Sci. U. S. A.* **2008**, *105*, 3668–3672.
[6] A. Bandyopadhyay, R. Pati, S. Sahu, D. Fujita, F. Peper, *Nat. Phys.* **2010**, *6*, 369–375.
[7] F. Ganazzoli, R. La Ferla, *J. Chem. Phys.* **2000**, *113*, 9288–9293.
[8] Gotlib, Yu. Ya, D. A. Markelov, *Poly. Sci. A* **2007**, *49*, 1137–1154.
[9] T. S. Elicker, D. G. Evans, *J. Phys. Chem. A* **1999**, *103*, 9423–9431.
[10] C. Devadoss, P. Bharathi, J. S. Moore, *J. Am. Chem. Soc.* **1996**, *118*, 9635–9644.
[11] S. D. Hudson, H.-T. Jung, V. Percec, W.-D. Cho, G. Johansson, G. Ungar, V. S. K. Balagurusamy, *Science* **1997**, *278*, 449–452.

[12] M. Garzoni, N. Cheval, A. Fahmi, et al. *J. Am. Chem. Soc.* **2012**, *134*, 3349–3357.
[13] R. Ju, M. Tessier, L. Olliff, R. Woods, A. Summers, Y. Geng, *Chem. Commun.* **2011**, *47*, 268–270.
[14] D. K. Yoon, S. R. Lee, Y. H. Kim, et al. *Physica B-Condensed Matter* **2006**, *385*, 801–803.
[15] J. F. G. A. Jansen, E. M. M. De Brabander-van Den Berg, E. W. Meijer, *Science* **1994**, *266*, 1226–1229.
[16] P. Carbone, F. Mueller-Plathe, *Soft Matter* **2009**, *5*, 2638–2647.
[17] K. Eric Drexler, *Trends Biotechnol.* **1999**, *17*, 5–7.
[18] V. Balzani, A. Credi, M. Venturi, in *Molecular Devices and Machines – A Journey into the Nanoworld*, Wiley-VCH Verlag GmbH & Co. KGaA, Weinheim **2003**.
[19] Nanoscience and nanotechnologies: opportunities and uncertainties, *The Royal Society & The Royal Academy of Engineering*, The Clyvedon Press, Cardiff, UK **2004**.
[20] G. Oshanin, A. Blumen, M. Moreau, S. F. Burlatsky, *J. Chem. Phys.* **1995**, *103*, 9864–9875.
[21] A. Bandyopadhyay, S. Sahu, D. Fujita, Wakayama Y. *Phys. Chem. Chem. Phys.* **2010**, *12*, 2033–2208.
[22] B. J. H. Mattews, A. C. Jones, N. K. Thedorou, A. W. Tudhope, *Marin. Chem.* **1996**, *55*, 317–332.
[23] E. Parlanti, B. Morin, L. Vacher, *Organ. Geochem.* **2002**, *33*, 221–236.
[24] V. Dierolf, M. Koerdt, *Phys. Rev. B* **2000**, *61*, 8043–8052.
[25] P. Andrew, W. L. Barnes, *Science* **2000**, *290*, 785–788.
[26] J. C. Johnson, H. Yan, P. Yang, R. J. Saykally, *J. Phys. Chem. B* **2003**, *107*, 8816–8828.
[27] A. M. Armani, A. Srinivasan, K. J. Vahala, *Nano Lett.* **2007**, *7*, 1823–1826.
[28] Y. Tsuboi, R. Shimizu, T. Shoji, N. Kitamura, *Anal. Sci.* **2010**, *26*, 1241–1245.
[29] S. Chénais, S. Forget, *Poly. Int.* **2012**, *61*, 390–406.
[30] D. A. Tomalia, *Aldrichchim. Acta* **2004**, *37*, 39–57.
[31] B. M. Kiran, N. Jayaraman, *Macromolecules* **2009**, *42*, 7353–7359.
[32] G. R. Newkome, V. V. Narayanan, L. Echegoyen, E. P. Cordero, H. Luftmann, *Macromolecules* **1997**, *30*, 5187–5191.
[33] M. Chai, A. K. Holly, M. Kruskamp, *Chem. Commun.* **2007**, *43*, 168–170.
[34] D. Kannaiyan, T. Imae, *Langmuir* **2009**, *25*, 5282–5285.
[35] J. Peterson, Allikmaa, V. J. Subbi, T. Pehk, M. Lopp, *Eur. Poly. J.* **2003**, *39*, 33–42.